

Atomic layer deposition of thin hafnium oxide films using a carbon free precursor

J. F. Conley, Jr.,^{a)} Y. Ono, D. J. Tweet, and W. Zhuang
Sharp Labs of America, Camas, Washington 98607

R. Solanki

Department of Electrical and Computer Engineering, Oregon Graduate Institute, Beaverton, Oregon 97006

(Received 29 April 2002; accepted 22 October 2002)

Thin HfO₂ films have been deposited on silicon via atomic layer deposition using anhydrous hafnium nitrate [Hf(NO₃)₄]. Properties of these films have been investigated using x-ray diffraction, x-ray reflectivity, spectroscopic ellipsometry, atomic force microscopy, x-ray photoelectron spectroscopy, and capacitance versus voltage measurements. Smooth and uniform initiation of film growth has been detected on H-terminated silicon surfaces. As-deposited films were amorphous, oxygen rich, and contained residual NO₃ and NO₂ moieties from the nitrate precursor. Residual nitrates were desorbed by anneals >400 °C, however, the films remained oxygen rich. Crystallization of thin films (<10 nm) occurred at roughly 700 °C. For films less than ~10 nm thick, the effective dielectric constant of the film and any interfacial layer (neglecting quantum effects) was found to be in the range of $k \sim 10-11$. From a plot of electrical thickness versus optical thickness, the dielectric constant of the HfO₂ layer was estimated to be $k_{\text{HfO}_2} \sim 12-14$. Leakage current was lower than that of SiO₂ films of comparable equivalent thickness. The lower than expected dielectric constant of the film stack is due in part to the presence of an interfacial layer (likely HfSiO_x). Excess oxygen in the films may also play a role in the reduced dielectric constant of the HfO₂ layer. © 2003 American Institute of Physics.
[DOI: 10.1063/1.1528306]

I. INTRODUCTION / BACKGROUND

Thermally grown SiO₂ has long been the gate dielectric of choice for metal-oxide-semiconductor (MOS) devices. However, due to an increase in the leakage current from direct tunneling (as well as boron penetration, reliability concerns, and other problems), SiO₂ may not be scaled much below 1.5 nm. For low power applications where high leakage currents cannot be tolerated, it is projected that a high dielectric constant replacement for SiO₂ will be needed by the 80 nm node in 2005.¹⁻³ Despite the compelling near term need, a suitable replacement still has not been determined, and it is likely to be more than 5 years before a high- k dielectric is ready for integration into advanced complementary MOS technologies.²

A class of materials being considered as alternate dielectrics are metal oxides (HfO₂, ZrO₂, Pr₂O₃, La₂O₃, Al₂O₃, etc.).^{1,4-22} Among these, HfO₂ is an excellent candidate due to a high bulk dielectric constant (κ), good thermal stability,⁴ and wide band gap and offsets.⁵ HfO₂ thin films deposited via sputtering, chemical vapor deposition (CVD), and atomic layer deposition (ALD) have shown potential.^{1,6-16,20-23}

One of the most promising deposition techniques is ALD.^{1,24-26} In ALD, precursors are introduced alternately into the deposition chamber. Reactions are self-limiting and take place on the substrate surface rather than above it. The

desired film is built up one monolayer at a time and the total deposited thickness is linearly dependent on the total number of deposition cycles. The self-limiting nature of the process allows for inherent atomic scale interfacial control and excellent conformality.

The ALD of HfO₂ has recently been demonstrated by alternately exposing substrate surfaces to vapors of HfCl₄ precursor and H₂O.^{9,10,25,26} Excellent uniformity and initiation of the deposition were reported on SiO₂ and Si₃N₄ surfaces. However, because an effective thickness <1.0 nm will be needed, it is desirable to avoid the use of low k layer and deposit the high- κ directly on H-terminated Si. It was found that the use of HfCl₄ precursor required an "incubation" period consisting of a number of ALD cycles to produce total coverage of a hydrogen-terminated Si surface.^{9,10} This difficulty of initiating deposition on H-terminated silicon can lead to a high degree of surface roughness. Moreover, metal tetrachlorides have a tendency to incorporate trace amounts of chlorine in the film, which can lead to stability and reliability problems. Use of a precursor that allows for better control of the initiation of deposition on H-terminated Si might aid in optimization of the interface properties and allow improvement of the carrier mobility in transistors.

A precursor that has generated much interest recently is the anhydrous nitrate of hafnium Hf(NO₃)₄.¹⁻¹³ Unlike metalorganic precursors, this precursor would not leave hydrocarbon or halogen impurities and the nitrogen oxide byproducts should be easily removable. It has been used in CVD

^{a)}Electronic mail: jconley@sharplabs.com

mode at temperatures from 300 to 500 °C to generate hafnium oxide films.^{12,13}

We report results of our investigation on the use of $\text{Hf}(\text{NO}_3)_4$ as a precursor for ALD of HfO_2 on H-terminated Si substrates. We find that the use of $\text{Hf}(\text{NO}_3)_4$ allows deposition of HfO_2 directly on H-terminated silicon without the need for an SiO_2 layer.²⁰ HfO_2 films were characterized using spectroscopic ellipsometry (SE), x-ray diffraction (XRD) and reflectivity, (XRR) x-ray photoelectron spectroscopy (XPS), atomic force microscopy (AFM), and electrical measurements.

II. EXPERIMENTAL DETAILS

Thin HfO_2 films were deposited using a Microchemistry F-120 traveling wave ALD reactor for 50 mm substrates, where the hafnium precursor was anhydrous hafnium nitrate [$\text{Hf}(\text{NO}_3)_4$]. Hafnium nitrate was synthesized by refluxing hafnium tetrachloride over dinitrogen pentoxide at 30 °C and then purified by sublimation at 110 °C and 0.1 mm Hg to yield white crystals.²⁷ Dinitrogen pentoxide was generated by reacting solid P_2O_5 and fuming nitric acid.²⁸ Vapors were trapped at liquid N_2 temperature into a reaction flask containing HfCl_4 . For deposition, the precursor temperature was set between 80 and 85 °C (based on measured thermal gravimetric analysis properties of the precursor).

Prime grade 150 mm *n*- and *p*-type (100) Si wafers of resistivity 4–30 or 4–10 Ω cm, respectively, were cleaned with standard SC-1 and SC-2 solutions and then cleaved into square pieces (5 cm on a side). To produce a H-terminated surface, the substrates were dipped into dilute HF solution immediately prior to film deposition. Since metal nitrate precursors such as $\text{Hf}(\text{NO}_3)_4$ easily decompose thermally, determination of the substrate temperature for ALD growth required optimization. A set of dummy runs was performed to grow thick films over a wide range of temperatures using only hafnium nitrate. The occurrence of CVD from thermal decomposition was detected by monitoring the film growth. The highest temperature at which thermal decomposition of $\text{Hf}(\text{NO}_3)_4$ was not observed was approximately 180 °C. At substrate temperatures below 180 °C, the introduction of alternate pulses of hafnium nitrate and water vapor resulted in the deposition of uniform films, an indication of the ALD regime. A typical ALD pulse sequence cycle was as follows: the first pulse is of metal nitrate (0.6 s), then a N_2 purge of 0.6 s, followed by a 0.6 s pulse of H_2O vapor, and finally a 0.6 s N_2 purge. This reaction sequence was repeated until the desired thickness was reached.

Film thickness and refractive index were determined using a Sentech SE-800 spectroscopic ellipsometer. A Cauchy film model was used to fit the refractive index of as-deposited thick films. For example, for an as-deposited 115.2 nm-thick HfO_2 film (deposited via 400 cycles of ALD), the following coefficients were obtained: $n_0 = 1.801$, $n_1 = 2.09 \times 10^4$, and $n_2 = -1.03 \times 10^9$, where $n(\lambda) = n_0 + n_1 \lambda^{-2} + n_2 \lambda^{-4}$, and λ is the wavelength in nanometers. At a λ of 632.8 nm, the real component of the refractive index, n , was found to be 1.847 ± 0.005 . The imaginary component, k , was zero, interpreted to indicate that the film was transparent. It

has been reported that as-deposited metal-rich sputtered thin HfO_2 films have a strong k component which can be reduced to zero by an oxygen anneal.²³

Electrical measurements were made on “dot” capacitors (approximately 100 μm radius, $\sim 3 \times 10^{-4} \text{ cm}^2$) formed by evaporating either Pt or Al through a shadow mask. High frequency (100 kHz and 1 MHz) capacitance versus voltage ($C-V$) measurements were made with a HP 4284 and $I-V$ with an HP4156A. The capacitive equivalent thickness (CET) of the HfO_2 films was estimated from C_{max} ($\text{CET} = k_{\text{SiO}_2} / C_{\text{max}}$) at 1 MHz. Since quantum effects are not accounted for, the CET can be considered more conservative than the effective oxide thickness (EOT) in which a correction is made (typically several angstroms) to account for quantum effects.

XRD and XRR measurements were performed using a Philips X’Pert system. XPS measurements were performed at a commercial laboratory²⁹ using a Physical Electronics Quantum 2000 with a monochromated Al $K\alpha$ (1486.6 eV) x-ray source. Surface roughness was measured with an AFM in the tapping mode.

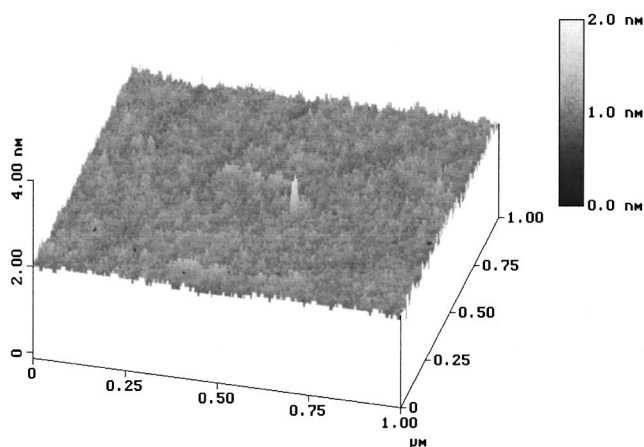
III. RESULTS AND DISCUSSION

A. Film deposition and morphology

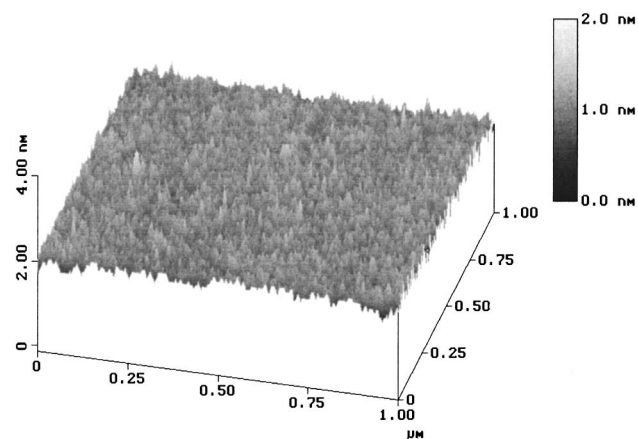
We found that ALD using $\text{Hf}(\text{NO}_3)_4$ precursor allowed initiation and smooth two-dimensional HfO_2 film growth directly on H-terminated Si surface starting with the first cycle. This is evident in Fig. 1 where AFM images are shown of HfO_2 films deposited after (a) one and (b) two ALD cycles. A control image (not shown) was recorded of the bare Si surface prior to deposition. rms roughness for the HfO_2 films was approximately 0.3 nm while rms roughness for the bare Si substrate was ~ 0.2 nm. For both depositions, a thin film covering the entire surface was detected by SE and XRR. The ease of initiation is an advantage over other precursors such as chlorides because of the potential for a minimal interfacial layer.

Since the $\text{Hf}(\text{NO}_3)_4$ precursor contains oxygen, thermal decomposition can produce HfO_2 without an oxidizing agent via a CVD reaction. However, for an ALD process, at least two reactants are required. Besides water, several alternate oxidizing reactants were also evaluated including $\text{C}_2\text{H}_5\text{OH}$, CH_3OH , $\text{C}_3\text{H}_7\text{OH}$, and H_2 . SE and electrical measurements indicated that, within the process parameter range of H_2O , these alternates did not produce a film.

Figure 2 shows a plot of optical thickness versus the number of deposition cycles for HfO_2 films deposited at 180 °C. A deposition rate of $\sim 0.12-0.14$ nm/cycle was observed over the range of deposition cycles. The deposition rate was sensitive to the condition of the deposition chamber, i.e., the amount of film deposited on the chamber walls, as well as substrate temperature and precursor temperature. A much higher deposition rate of 0.36 nm/cycle that was initially reported in Ref. 20 has been traced to cleaning of the furnace chamber. Films deposited following cleaning were found to exhibit higher deposition rates than those deposited subsequently. Although at this time there is not conclusive evidence as to the mechanism of the enhanced deposition



(a)



(b)

FIG. 1. AFM images of HfO_2 films deposited via one (a) and two (b) ALD cycles.

rate, one possible explanation may be moisture released from the cleaned surface triggering a CVD growth component during the $\text{Hf}(\text{NO}_3)_4$ ALD cycles. More careful control of the deposition conditions has since resulted in lower and better controlled deposition rates, more consistent with those typically reported for ALD.

X-ray diffraction and reflectivity measurements were made on a thick (127 nm, via XRD) HfO_2 film. As shown in Fig. 3, an XRD phase scan revealed no sharp peaks, indicat-

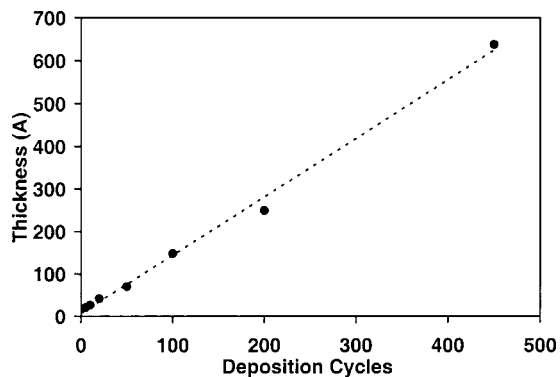


FIG. 2. Plot of HfO_2 thickness vs number of ALD cycles.

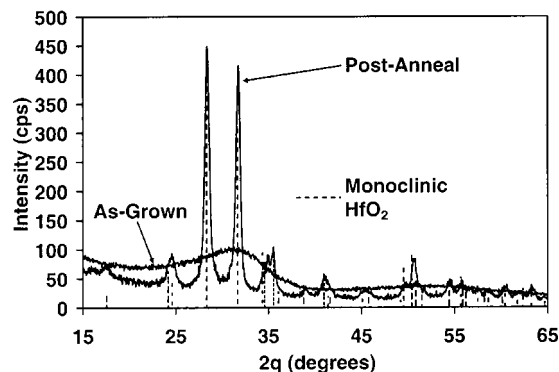


FIG. 3. XRD phase spectra of a 400 cycle HfO_2 film, as-deposited and after a 300 s anneal in N_2 at 850 °C.

ing that the as-deposited film is likely amorphous. An amorphous phase is desirable since one might expect less leakage current due to lack of grain boundaries. A 850 °C anneal in N_2 for 300 s resulted in conversion to a polycrystalline phase. The sharp peaks of the postanneal XRD phase scan (Fig. 3) indicate a monoclinic phase with $\sim 30\text{--}40$ nm crystallites. (The vertical lines in Fig. 3 represent the powder diffraction pattern for monoclinic HfO_2 .)³⁰

XRR spectra for the same film are shown in Fig. 4. Theoretical modeling of the as deposited film indicated a thickness of 127.5 ± 1.0 nm, a density of 6.7 ± 0.1 g/cm³, a surface roughness of ~ 0.8 nm rms, and a Si substrate roughness of ~ 0.3 nm rms. The high number of oscillations reflect the excellent uniformity of the film over the ~ 10 mm \times 20 mm beam size. Analysis of the postanneal reflectivity spectrum indicated a 98.5-nm-thick film with a density of 8.5 ± 0.1 g/cm³, a roughness of 1.2 nm rms, and a Si substrate roughness of 0.45 nm rms, suggesting that, in addition to crystallization, the anneal also densified the film. SE measurements indicated that the anneal resulted in a decrease in thickness from 115.2 to 100.3 nm and an increase in n from 1.847 ± 0.005 to 1.899 ± 0.005 , consistent with densification. As these films were deposited at 180 °C, the densification was not surprising. High temperature anneals are routinely used to densify oxides deposited at lower temperatures. It is interesting to note that even after the anneal (850 °C, 30 s), the density of the thin film was less than the value reported for bulk HfO_2 (9.68 g/cm³).³¹

XRD spectra of thin (~ 4.1 nm) HfO_2 films annealed for $\sim 1\text{--}5$ min at roughly 50 °C increments starting at 400 °C

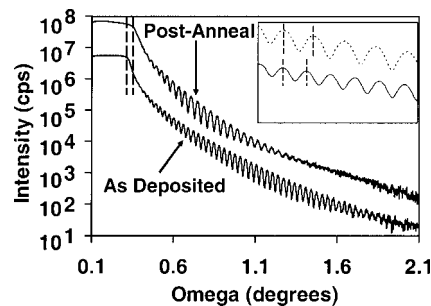


FIG. 4. X-ray reflectivity spectra of a 400 cycle HfO_2 film, as-deposited and after a 300 s anneal in N_2 at 850 °C (inset shows uniformity of oscillations).

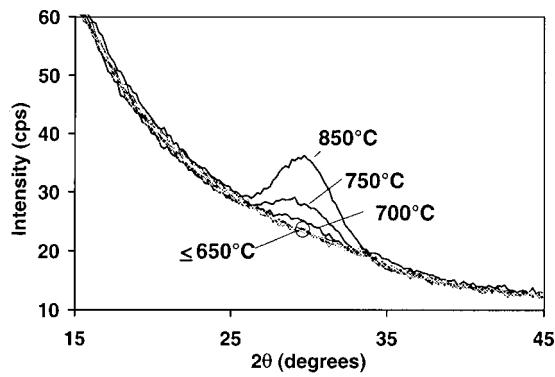


FIG. 5. XRD phase spectra of a thin (~ 4.1 nm) HfO_2 film annealed at various temperatures. The 850°C spectrum was taken using a 5.1 nm-thick film. Onset of crystallization occurs at $\sim 700^\circ\text{C}$.

are shown in Fig. 5. The films showed onset of crystallization at 700°C with peak strengthening at 750°C . (The spectrum labeled 850°C was taken using a ~ 5.1 nm film.) A single broad peak was detected at $2\theta \sim 30^\circ$, centered approximately between the two largest monoclinic phase peaks. We were unable to positively identify the phase responsible for this peak. XRR and SE modeling indicated that densification occurred at the lowest temperature used (400°C) and that relatively little change occurred with subsequent anneals. The $\sim 700^\circ\text{C}$ crystallization temperature is consistent with that reported by Lee *et al.* for dc magnetron sputtered HfO_2 , and suggests that ALD of HfO_2 using $\text{Hf}(\text{NO}_3)_4$ is compatible with the anticipated thermal budget of replacement gate technology. Other groups have reported different crystallization temperatures for different deposition methods and thicknesses of HfO_2 . For example, CVD films deposited at 450°C were reported to be monoclinic¹¹ and ~ 3 nm films deposited via jet vapor deposition showed onset of crystallization between 400 and 500°C .¹⁴ It is well known that the properties of SiO_2 depend strongly on the deposition method and it is likely that the properties of HfO_2 are also deposition method dependent.¹¹

XPS was performed on a (4.1 nm) ALD HfO_2 sample before and after a 30 s, 450°C forming gas anneal. The analysis determined that the main constituents of the as-deposited film were oxygen (62.3 at. %) and hafnium (16.1%), indicating an oxygen rich film. CVD HfO_2 films deposited at 450°C using $\text{Hf}(\text{NO}_3)_4$ were also reported to be O rich, with O to Hf ratio increasing at lower deposition temperatures.¹¹ Other elements detected were carbon (13.8%) which was surface contamination, silicon (5%) presumably from the substrate, fluorine (0.7%) from the HF last clean, zirconium (0.9%) which is inherently contained in the hafnium source, and nitrogen (1.2%), in the form of NO_3 and NO_2 , from the nitrate precursor. The residual nitrogen ligands were eliminated by light sputtering of the surface, an indication that a film of ligands may remain on the surface after the final deposition cycle. A thin silicon-rich HfO_2 layer (likely silicate) was also detected. We were not able to determine the exact composition of this layer. The silicate layer was not removed by light sputtering of the surface suggesting that it may reside near the interface.

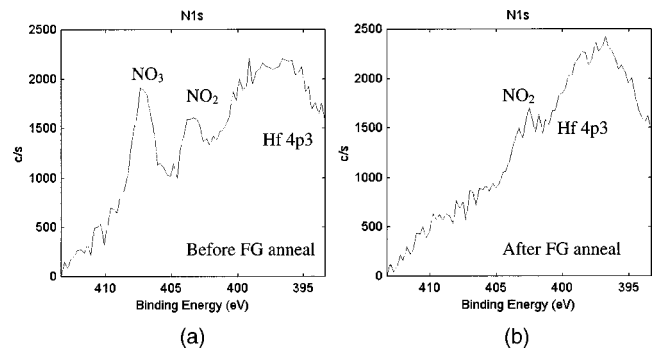


FIG. 6. XPS spectra of nitrogen related peaks (a) before and (b) after a 30 s anneal at 450°C in forming gas.

The forming gas anneal resulted in a reduction in nitrogen content to 0.2% and a small reduction in oxygen to hafnium ratio to 2.76 . A high resolution XPS scan of the nitrogen bonding, shown in Fig. 6, indicated that the residual nitrogen from the precursor ligands [Fig. 6(a)] was eliminated by the 450°C anneal [Fig. 6(b)], suggesting that a low temperature postdeposition anneal should be effective. This loss of oxygen and nitrogen may account for the anneal induced densification and decrease in thickness that was observed via x-ray reflectivity and spectroscopic ellipsometry. The amount of silicate was unchanged by the anneal.

B. Electrical measurements

A 1 MHz capacitance versus voltage trace of a ~ 5.7 -nm-thick p -type HfO_2 capacitor with a Pt electrode is shown in Fig. 7. This sample was annealed after metallization for 60 s in 5% H_2 (N_2 balance) at 400°C . The CET of this film, including the interfacial layer, was estimated to be ~ 2.1 nm (at $V_g = -2.0$ V), corresponding to an effective dielectric constant of $\kappa_{\text{eff}} \sim 10.5$ (κ_{eff} includes the interfacial layer). CET was determined from C_{max} at 1 MHz. It was found that a postmetallization forming gas anneal (PMA) dramatically improved $C-V$ characteristics, reducing interface trap density and hysteresis, and increasing C_{max} . Although C_{max} increased, κ remained roughly unchanged, likely due to the decrease in thickness of the film due to densification (as indicated by SE and XRR).

A set of 1 MHz $C-V$ traces of an as-deposited ~ 5.8 nm HfO_2 film over the course of a series of sequential 15 s

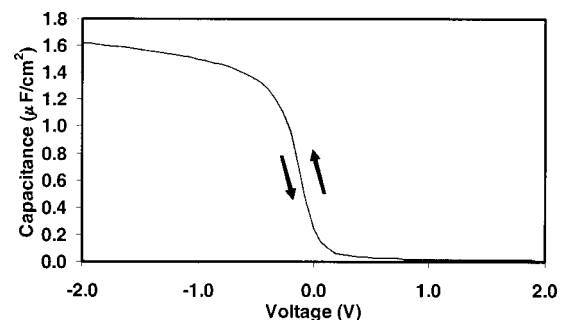


FIG. 7. 1 MHz capacitance vs voltage trace of a ~ 5.7 -nm-thick Pt HfO_2 capacitor on p -type Si after a 60 s postmetallization anneal in 5% H_2 in N_2 at 400°C .

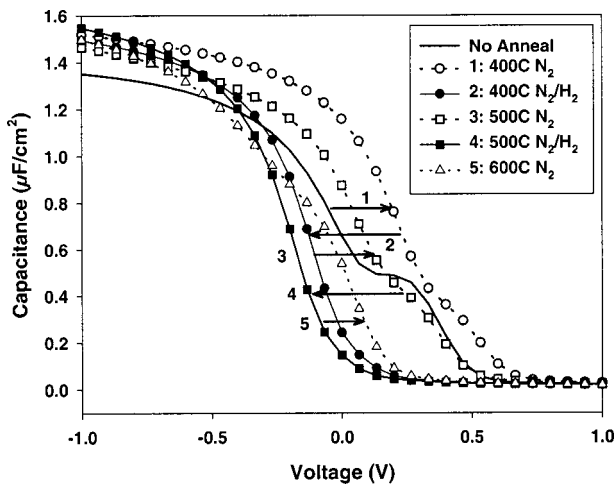


FIG. 8. Capacitance vs voltage traces for the anneal sequence consisting of (1) 400 °C in N_2 , (2) 400 °C in N_2/H_2 , (3) 500 °C in N_2 , (4) 500 °C in N_2/H_2 , and (5) 600 °C in N_2 .

duration PMAs is shown in Fig. 8. (The film did not receive a postdeposition anneal.) The anneal sequence was designed to qualitatively assess the effects of various postdeposition anneal treatments and consisted of: (1) 400 °C in N_2 , (2) 400 °C in N_2/H_2 , (3) 500 °C in N_2 , (4) 500 °C in N_2/H_2 , and (5) 600 °C in N_2 . The film remained amorphous after this sequence. A dielectric constant of approximately 10–11, and a CET between 2.0 and 2.3 nm was extracted for this film. Figure 9 shows hysteresis for a ± 2 V sweep as a function of annealing conditions. The initial 400 °C anneal in N_2 reduced interface trap density and hysteresis, resulted in a $\sim 10\%$ increase in C_{max} , and caused a positive shift in the flatband voltage. C_{max} did not significantly change after this initial anneal. The subsequent 400 °C N_2/H_2 anneal further reduced interface trap density, eliminated hysteresis, and produced a negative shift in flatbands. A subsequent 500 °C anneal in N_2 visibly increased interface trap density and resulted in a positive shift in the flatband voltage. The following 500 °C anneal in N_2/H_2 again reduced interface trap density and caused a negative shift in flatband voltage. The final 600 °C anneal in N_2 increased interface trap density and produced a positive shift in flatband voltage. From Figs. 8 and 9, it is seen that a 400 °C anneal in N_2/H_2 was sufficient

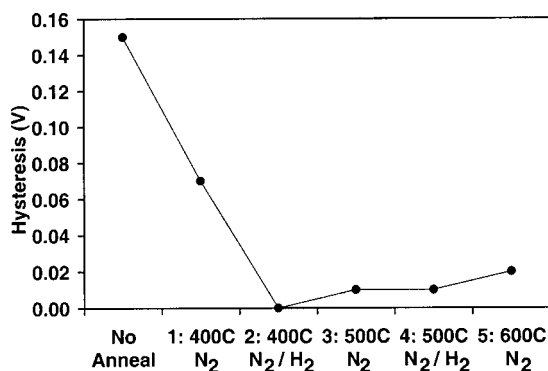


FIG. 9. Plot of CV hysteresis for anneal sequence consisting of (1) 400 °C in N_2 , (2) 400 °C in N_2/H_2 , (3) 500 °C in N_2 , (4) 500 °C in N_2/H_2 , and (5) 600 °C in N_2 .

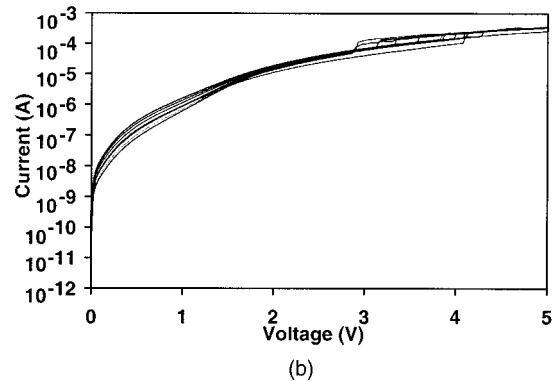
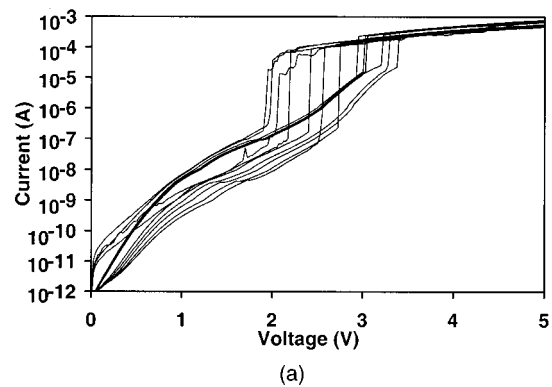


FIG. 10. Current vs voltage for (a) HfO_2 (CET=2.2 nm), and (b) SiO_2 (optical thickness=2.0 nm).

to eliminate hysteresis and reduce interface trap density. For all temperatures, the use of a N_2/H_2 ambient produced lower hysteresis, interface trap density, and flatband voltage shift than a N_2 -only ambient. This result suggests that, as in SiO_2 , H plays a role in passivating electrically active defects in HfO_2 . Recent electron spin resonance (ESR) results demonstrate that H anneals passivate Si dangling bonds at the HfO_2/Si interface.³²

A simple voltage ramp test was conducted to obtain a rough estimate of breakdown (BD) strength. The test was performed on an HP4156A with the integration time set to medium (20 ms), a ramp rate was not specified. Capacitors were biased in accumulation. Figure 10 shows a plot of current versus voltage for (a) HfO_2 (CET ~ 2.2 nm), and (b) SiO_2 (SE thickness ~ 2.0 nm). At $V_g = 1$ V, lower leakage is observed in the HfO_2 film than in the SiO_2 film of similar CET. Harder breakdowns were observed in the physically thicker HfO_2 films. Some of the scatter in the leakage and breakdown data may be due to the nonuniformities inherent in the shadow mask capacitor formation process as well as the relatively large area of the dots. A comparison of BD characteristics of these samples is shown in Fig. 11. The breakdown strength of the HfO_2 was approximately 5–7 MV/cm while that of the SiO_2 was >15 MV/cm. Fields were determined using the optical thickness (SE). A forming gas anneal (“diamond” symbols) slightly degraded the breakdown strength of the HfO_2 . The test probe makes contact directly over the oxide being tested. Since it is well known that probe pressure has an impact on breakdown of SiO_2 , it is likely that probe pressure effects may have con-

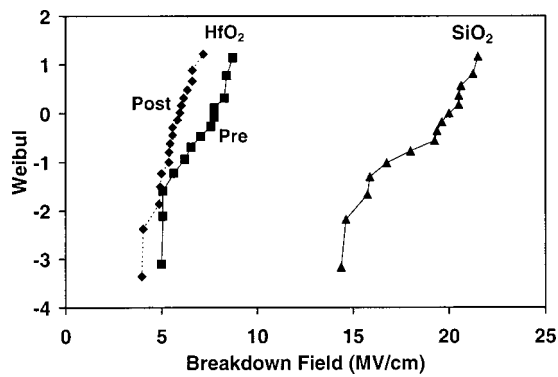


FIG. 11. Voltage ramp breakdown comparison of HfO₂ (pre- and post-anneal) and SiO₂.

tributed to reducing the breakdown voltages reported here for HfO₂. Probe pressure was not monitored. It is likely that more carefully controlled testing on structures with a remote contact would produce higher breakdown voltages for HfO₂.

In an effort to obtain a more accurate assessment of κ , CV measurements were made on a series of HfO₂ films of various thicknesses. Figure 12 shows a plot of CET versus optical thickness for the HfO₂ films in Fig. 1. As expected, the electrical thickness of the films decreases as the physical thickness decreases. We assume that (1) the HfO₂ film is a stack consisting of a HfO₂ layer on top of an interfacial layer (IL) and (2) the structure and thickness (d_{IL}) of this interfacial layer are independent of the HfO₂ film thickness. From the slope of the plot, we extract $k_{\text{HfO}_2} \sim 12-14$. Assuming $k_{\text{IL}} = 3.9$, we extract $d_{\text{IL}} \sim 0.5-1.0$ nm from the intercept. These results suggest that even though Hf(NO₃)₄ allows initiation of ALD directly on H-terminated Si, formation of an interfacial layer still occurs. The exact thickness and chemical composition of the interfacial layer are not definitively known. Likely candidates include SiHfO_x and SiO₂. As mentioned earlier, XPS analysis points to the presence of an interfacial silicate layer. Recent electron spin resonance results on these films appear to rule out the presence of pure SiO₂ at the interface.³²

The dielectric constant range of 10–11 extracted for the thin HfO₂ films in Figs. 7 and 8 is lower than that reported for bulk HfO₂ ($\kappa = 25-30$).¹ There are several reasons why the thin film dielectric constant might be expected to be

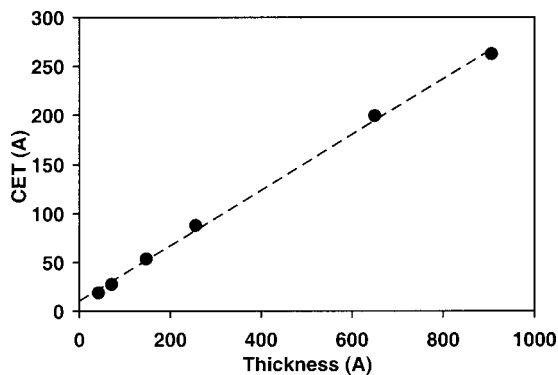


FIG. 12. Plot of CET vs thickness measured via spectroscopic ellipsometry.

lower than the bulk value. (The reduced κ cannot be accounted for by the reduction of effective dielectric constant that is theoretically predicted in ultrathin, ultrahigh- κ films.³³) First, the CET estimate is conservative, neglecting substrate quantum effects which, if taken into account, would reduce the estimated thickness by 0.2–0.3 nm and correspondingly increase κ . Second, as indicated in Fig. 12, a thin interfacial layer is present which effectively reduces the overall κ value. Finally, as also indicated in Fig. 12, the κ of HfO₂ layer itself is lower than that of bulk material. The refractive index and density are also both lower than the reported bulk. The detection by XPS of excess oxygen raises the possibility that excess oxygen plays a role in reducing the “bulk” κ of the HfO₂ layer. This suggests that in order to obtain a thinner CET, it may be necessary to reduce the oxygen content and increase film density as well as reducing the thickness of the interfacial layer.

Despite the apparently low value of κ for the HfO₂ layer and the presence of an interfacial layer, our results are consistent with recently reported results for thin HfO₂ gate oxide stacks. Hobbs *et al.*¹⁵ recently reported a CET of 2.5 nm for a 4.2 nm HfO₂ stack deposited via metalorganic CVD, corresponding to a conservative $k_{\text{stack}} \sim 6.6$. A transmission electron microscopy revealed that their gate stack consisted of a 3.0 nm layer of HfO₂ and a 1.2 nm interfacial layer. Kim *et al.*,¹⁶ recently reported an EOT of 1.7 nm for a 4.6 nm HfO₂ stack deposited via ALD (precursor not indicated) corresponding to a (nonconservative) $\kappa \sim 10.6$ for their stack.

IV. SUMMARY AND CONCLUSION

Films produced using anhydrous hafnium nitrate [Hf(NO₃)₄] as a precursor for ALD of HfO₂ have been investigated using x-ray diffraction, x-ray reflectivity, spectroscopic ellipsometry, atomic force microscopy, x-ray photoelectron spectroscopy, and capacitance versus voltage measurements. It was found that the use of Hf(NO₃)₄ allows initiation directly on a H-terminated Si surface. A uniform and smooth film covering the entire surface of a H-terminated Si wafer was detected after only a single cycle deposition. XRD, XRR, SE, and AFM analysis indicated that as-deposited films were uniform and amorphous. XPS analysis indicated that the as-deposited films were oxygen rich and contained silicate (likely at the interface) and residual NO₃ and NO₂ from precursor ligands. A 400 °C anneal resulted in densification and elimination of the residual N content, but did not change the silicate layer. Onset of crystallization occurred at approximately 700 °C.

Electrical measurements indicated that HfO₂ films had lower leakage than SiO₂ of similar EOT, but also lower BD strength. A 400 °C rapid thermal annealing in H₂/N₂ reduced interface trapping and hysteresis. For HfO₂ films (including interfacial layers) less than ~ 15 nm thick, a dielectric constant in the range of 10–11 was estimated. This estimate neglects quantum effects which if accounted for would result in an increased effective dielectric constant. The lower than expected dielectric constant is due partially to the presence of an interfacial layer such as silicate or SiO₂. Recent ESR results indicate that the interfacial layer is not pure

SiO₂.³² A lower than expected dielectric constant of 12–14 was extracted for the HfO₂ layer. Excess O (HfO_x, where $x > 2$, as detected by XPS) as well as reduced film density may play a role in reducing the dielectric constant of the “bulk” HfO₂ layer.

Overall, ALD of HfO₂ using Hf(NO₃)₄ looks promising. Optimization of deposition parameters and postdeposition annealing, perhaps to reduce O content and/or increase film density, will likely result in improved leakage, capacitance, and equivalent thickness.

ACKNOWLEDGMENTS

The authors wish to thank B. Meyer for AFM images and S. K. Mohammed for assistance with film depositions.

- ¹G. D. Wilk, R. M. Wallace, and J. M. Anthony, *J. Appl. Phys.* **89**, 5243 (2001).
- ²International Technology Roadmap for Semiconductors, 2001, <http://public.itrs.net/Files/2001ITRS/Home.htm>.
- ³M. L. Green, E. P. Gusev, R. Degraeve, and E. L. Garfunkel, *J. Appl. Phys.* **90**, 2057 (2001).
- ⁴K. J. Hubbard and D. G. Schlom, *J. Mater. Res.* **11**, 2757 (1996).
- ⁵J. Robertson, *J. Vac. Sci. Technol. B* **18**, 1785 (2000).
- ⁶B. H. Lee, L. Kang, W. J. Qi, R. Nieh, Y. Jeon, K. Onishi, and J. C. Lee, *Tech. Dig.-Int. Electron Devices Meet.* **1999**, 133 (1999).
- ⁷B. H. Lee, L. Kang, R. Nieh, W. J. Qi, and J. C. Lee, *Appl. Phys. Lett.* **76**, 1926 (2000).
- ⁸T. Ma *et al.*, *IEEE Trans. Electron Devices* **48**, 2348 (2001).
- ⁹M. Copel, M. Gribelyuk, and E. Gusev, *Appl. Phys. Lett.* **76**, 436 (2000).
- ¹⁰G. D. Wilk *et al.*, *IEEE 2002 Symp. on VLSI Tech. Dig. of Tech Papers*, p. 28-29 (2002).
- ¹¹R. C. Smith *et al.*, *Adv. Mater. Opt. Electron.* **10**, 105 (2000).
- ¹²D. G. Colombo, D. C. Gilmer, V. G. Young, S. A. Campbell, and W. L. Gladfelter, *Chem. Vap. Deposition* **4**, 220 (1998).
- ¹³J. Park, B. K. Park, M. Cho, C. S. Hwang, K. Oh, and D. Y. Yang, *J. Electrochem. Soc.* **149**, G89 (2002).
- ¹⁴W. Zhu, T. P. Ma, T. Tamagawa, Y. Di, J. Kim, R. Carruthers, M. Gibson, and T. Furukawa, *Tech. Dig.-Int. Electron Devices Meet.* **2001**, 463 (2000).
- ¹⁵C. Hobbs, *et al.*, *Tech. Dig.-Int. Electron Devices Meet.* **2001**, 651 (2001).
- ¹⁶Y. Kim *et al.*, *Tech. Dig.-Int. Electron Devices Meet.* **2001**, 455 (2001).
- ¹⁷S. Jeon, K. Im, H. Yang, H. Lee, H. Sim, S. Choi, T. Jang, and Y. Hwang, *Tech. Dig.-Int. Electron Devices Meet.* **2001**, 471 (2001).
- ¹⁸Y. Ma, Y. Ono, L. Stecker, D. R. Evans, and S. T. Hsu, *Tech. Dig.-Int. Electron Devices Meet.* **1999**, 149 (1999).
- ¹⁹H. Zhang and R. Solanki, *J. Electrochem. Soc.* **148**, 63 (2001).
- ²⁰J. F. Conley, Jr., Y. Ono, D. J. Tweet, W. Zhuang, W. Gao, M. S. Kaiser, and R. Solanki, *Electrochem. Solid-State Lett.* **5**, C57 (2002).
- ²¹R. Gordan, J. Becker, D. Hausmann, and S. Suh, *Chem. Mater.* **13**, 2463 (2001).
- ²²J. F. Conley, Jr., Y. Ono, D. J. Tweet, W. Zhuang, and R. Solanki, *Mater. Res. Soc. Symp. Proc.* **716**, B2.2.1-6 (2002).
- ²³E. P. Gusev *et al.*, *Proc. of the ECS Meeting*, Abstract No. 578, March 2001.
- ²⁴T. Suntola, *Mater. Sci. Rep.* **4**, 261 (1989).
- ²⁵M. Ritala, M. Leskela, L. Niinisto, T. Prohaska, G. Friedbacher, and M. Grassbauer, *Thin Solid Films* **249**, 155 (1994).
- ²⁶M. Tuominen, T. Kanninen, and S. Haukka, *Electrochemical Society Proceedings* **2000-9**, 271 (2000).
- ²⁷B. O. Field and C. J. Hardy, *Proc. Chem. Soc.* **76**, (1962).
- ²⁸W. Zhuang, J. F. Conley, Y. Ono, D. R. Evans, and R. Solanki, *Integr. Ferroelectr.* (accepted).
- ²⁹G. Stossman, C. Evans, and Assoc. (private communication).
- ³⁰JCPDS, 34-0104 (1996).
- ³¹*CRC Handbook of Chemistry and Physics*, 77th ed., edited by D. R. Lide, (CRC Press, New York, 1996), pp. 4–60.
- ³²A. Kang, P. M. Lenahan, J. F. Conley, Jr., and R. Solanki, *Appl. Phys. Lett.* **81**, 1128 (2002).
- ³³K. Natori, D. Otani, and N. Sano, *Appl. Phys. Lett.* **73**, 632 (1998).